

FLOW SEPARATION CHARACTERISATION OF A FORWARD FACING STEP IMMERSED IN A TURBULENT BOUNDARY LAYER

Michael John Sherry, David Lo Jacono, John Sheridan
Fluids Laboratory for Aerospace and Industrial Engineering,
Department of Mechanical and Aerospace Engineering,
Monash University, Victoria, 3800, Australia
michael.sherry@eng.monash.edu.au

Romain Mathis, Ivan Marusic
Walter Basset Aerodynamic Laboratory,
Department of Mechanical Engineering
University of Melbourne, Victoria, 3010 Australia

ABSTRACT

Flow separation experiments are conducted in two facilities using particle image velocimetry (PIV) and pressure tappings over a wide Reynolds number range for a forward facing step immersed in a turbulent boundary layer. Bluff body flow is observed with the fixed separation point located at the leading edge of the model. The recirculation region dimensions are characterised over the entire Reynolds number range using the PIV technique. Pressure tappings provide insight into the surface pressure distribution in a recirculation region. The mechanisms affecting the reattachment distance, X_L , namely the turbulent mixing within the boundary layer and the velocity deficit in the boundary layer are commented on.

INTRODUCTION

Separating and reattaching flow phenomena are of particular interest in the wind engineering field. One area of wind engineering which has seen rapid development in recent times is the wind energy field. Wind generating machines or turbines are commonly sited in the vicinity of topological features such as coastal cliffs and escarpments in the atmospheric surface layer due to localized wind speed up effects the feature produces. The current one-dimensional numerical models the wind industry utilises in the planning process are unable to predict flow separation. Turbines placed within the recirculation region atop a cliff will be subjected to fluctuating loads and high vertical shear forces. Optimal placement beyond the highly distorted recirculation region will ensure increased power production whilst not subjecting the turbine to unknown fluctuating loads.

There has been a number of works dealing with obstacles immersed in turbulent boundary layers. The majority have concentrated on flow over a backward facing step and a comprehensive review of these studies can be found in Eaton and Johnston (1981). Studies dealing with separating and reattached flow over a forward facing isolated step (FFS) are less numerous probably due to the presence of two recirculation regions. In addition researchers also face difficulty in obtaining accurate data in the recirculation region and attributing flow behaviour to an individual flow parameter due to the dependence of results on numerous flow parameters (Bradshaw and Wong 1972). The flow over a FFS has numerous unique features which are shown in figure 1. The turbulent boundary layer approaches the obstacle from left

to right. As the pressure gradient due to the blockage of the step increases upstream, an adverse pressure gradient forms. The flow separates at $\sim 1-1.2h$ upstream and reattaches to the vertical step wall at $\sim 0.6h$ above the ground surface (Leclercq et al., 2001). The upstream recirculation region contains near stagnant fluid which acts as an 'equivalent' slope angle (Bowen and Lindley, 1977).

The blunt leading edge of the forward facing step acts as the sole fixed separation point for this geometry. A recirculation occurs behind the step, extending from the leading edge to the reattachment point, denoted as X_L . Hence, a strong shear layer develops between the low velocity adverse flow close to the wall and the mean free stream flow, increasing local mixing and turbulent intensity within the boundary layer. In the case of a blunt flat plate (i.e. $\delta/h \gg 1$), the free stream turbulence level significantly influences the reattachment length although its mechanism is unclear (Hillier and Cherry, 1981). The vorticity within the free shear layer periodically rolls up creating vortices which move downstream and dictate the instantaneous reattachment position (Kiya and Sasaki, 1983). These structures induce a low frequency oscillation of the shear layer, accompanied by an ejection of fluid from the recirculation region. Therefore, the unsteady behaviour of the shear layer implies that the reattachment point also fluctuates (within a 'reattachment zone' as shown in figure 1).

The mean reattachment position, X_L , is sensitive to certain parameters, such as the streamwise length to step height ratio, L/h and the upstream boundary layer thickness to step height ratio δ/h (Castro, 1979). A sufficiently large model L/h ratio is also required to consider the step truly 'isolated'. It has been shown that the three dimensionality of the recirculation region increases with reductions in the spanwise width to step height ratio, W/h (Largeau and Moriniere, 2007). A single dominant parameter affecting X_L

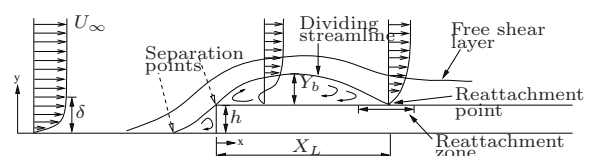


Figure 1: Flow features over a forward facing step

Table 1: Reattachment length results from previous researchers

Study	δ/h	L/h	Re_h	X_L
Largeau and Moriniere (2007)	≤ 0.3	≥ 9	$2.88-12.82 \times 10^4$	$3.5-5h$
Bergeles and Athanassiadis (1983)	0.48	4	2.7×10^4	$3.75h$
Moss and Baker (1980)	0.7	12.7	5×10^4	$4.7h$
Gasset et al. (2005)	~ 0.7	> 6	5×10^4	$5.0h$
Zhang (1994)	0.7	32	-	$4.02h$
Leclercq et al. (2001)	0.7	10	1.7×10^5	$3.2h$
Current Study	0.9-4	≥ 11.1	$2-20 \times 10^3$	$1.1-4h$
Arie et al. (1975)	1.96	4	-	$2.5h$
Farrabee and Casarella (1986)	2.4	> 10	2.1×10^4	$\sim 3h$
Camussi et al. (2008)	5	> 8	$8.8-26.3 \times 10^3$	$1.5-2.1h$
Castro and Dianat (1983)	5.2	2	5×10^4	$1.4h$
Agelinchaab and Tachie (2008)	9.3	6	1.92×10^3	$4.1h$

is difficult to determine due to the complex coupled relationship between the two separated region involved in the FFS geometry.

The previous recirculation studies involving a forward facing step immersed in a turbulent boundary layer can broadly be separated into two categories, those which have $\delta/h > 1$ and those with $\delta/h < 1$. Studies conducted with $\delta/h > 1$ have clearly shown the reattachment length is heavily dependant on δ/h (Agelinchaab and Tachie, 2008; Camussi et al., 2008; Farabee and Casarella, 1986; Castro and Dianat, 1983; Arie et al., 1975), whereas when $\delta/h < 1$ it seems that the reattachment length is weakly affected by this ratio, and usually situated around $4h$ to $5h$ (Largeau and Moriniere, 2007; Zhang, 1994; Bergeles and Athanassiadis, 1983; Moss and Baker, 1980). Results from previous researchers are summarised in table 1. The purpose of this study is to investigate the behaviour of a forward facing step immersed in a turbulent boundary layer for various δ/h ratios.

EXPERIMENTAL SETUP

The experiments were performed in two facilities, the FLAIR recirculating water channel at Monash University and the low speed boundary layer wind tunnel at the Walter Basset Aerodynamic laboratory at the University of Melbourne. The water channel was used for the PIV studies whereas pressure measurements were made in the wind tunnel. The two experimental facilities and models will be described separately below.

Water channel. The FLAIR water channel has a working section of $600 \times 800 \times 4000$ mm and a working speed range of $0.09 \text{ m/s} < U_\infty < 0.46 \text{ m/s}$. The channel walls are constructed of glass allowing easy optical access. Flow uniformity is achieved through the use of an upstream honeycomb section and fine turbulence screen. The flow passes through a 3:1 contraction to accelerate the mean flow and reduce the residual streamwise turbulence intensity to 1%.

The experiments were conducted over a wide Reynolds number range, $2000 < Re_h < 20000$ based on the definition given in equation 1. The flow passes through an additional turbulence screen situated 250 mm upstream of the leading edge of the model and serves to regulate the turbulence level at 1.43% between subsequent measurement days.

$$Re_h = \frac{U_\infty h}{\nu} \quad (1)$$

where U_∞ is the free stream velocity, h is the step height, and ν is the kinematic viscosity of the working fluid.

A Nd:YAG laser was used to produce a pulsed light sheet 2 mm thick. The flow was seeded with reflective polyamide particles of mean diameter $50 \mu\text{m}$ and specific gravity of 1.06 g/cm^3 .

A PIV camera of maximum resolution 4008×2672 pixels was used in conjunction with an 200 mm lens. A minimum magnification factor (MF) of 50 pixels/mm was utilised giving a field of view (FOV) of $40 \text{ mm} \times 26 \text{ mm}$. This allowed an instantaneous velocity map of 125 by 83 vectors to be captured when the minimum binning function on the camera was utilised. This FOV required the camera to be traversed back across the top of the step to capture the entire recirculation region. The camera was re-positioned using a manual traversing mechanism with camera alignment ensured prior to data acquisition. Validated cross correlation PIV software developed in-house was employed to generate the pif files (Fouras et al., 2008).

The experimental model was constructed of acrylic and polycarbonate for rigidity. The step height, h , was varied from 15 to 45 mm through the use of perspex spacers giving an aspect ratio range based on model width to step height of $11.1 < AR < 33.3$. The model aspect ratios, L/h and W/h , were above the critical aspect ratios determined by previous researchers to ensure reattachment to the top surface for every flow setting and nominally two dimensional flow at mid span respectively (Castro and Dianat, 1983; de Brederode and Bradshaw, 1972).

The model was fitted with end plates to minimise 3D edge effects and all edges bar the FFS leading edge were formed into an asymmetric 5° taper to minimise blockage effects. The maximum blockage ratio ($h = 45 \text{ mm}$) in the current tests was 9.73%. No corrections were made to adjust the results due to blockage affects.

A boundary layer formed upstream of the step with the profile as shown in figure 2. The boundary layer has a thickness $\delta = 2.7h_{h=15 \text{ mm}}$ measured at a distance $9h_{h=15 \text{ mm}}$ upstream of the step. The different step heights gave a δ/h range of $0.9 < \delta/h < 2.7$. The influence of this upstream boundary layer will be discussed later in the paper.

Wind tunnel. The low speed boundary layer wind tunnel is a suck down open type wind tunnel. The tunnel has a working section of $1200 \times 900 \times 6000$ mm with a maximum speed of $U_\infty = 3.4 \text{ m/s}$. The Reynolds number range tested in the wind tunnel was $2500 < Re_h < 4300$. The inlet

flow passes through several turbulence screens of differing scale to reduce residual turbulence levels. The boundary layer was tripped at the start of the test section by a 6 mm rod. The turbulent boundary layer profile was measured using a pitot tube attached to an automated traverse. The boundary layer thickness was approximately $\delta = 4h_{h=19mm}$ at all Reynolds numbers tested with a shape factor ranging from $1.4 < H < 1.5$. The turbulent boundary layer profiles are shown in figure 2.

The model used within the wind tunnel was constructed of a 19 mm ply wood board with a stainless steel plate containing 150 pressure tap holes flush mounted into the top surface. The model was placed 4.8 m from the tunnel inlet and hence boundary layer trip. The model spanned the entire working section of the wind tunnel. The model height can be adjusted. However, to date only the minimum step height has been tested producing a δ/h ratio of 4. Pressure measurements were obtained using a MKS Baratron 10 Torr pressure transducer. The pressure signals were passed through a MKS type 270 signal conditioner.

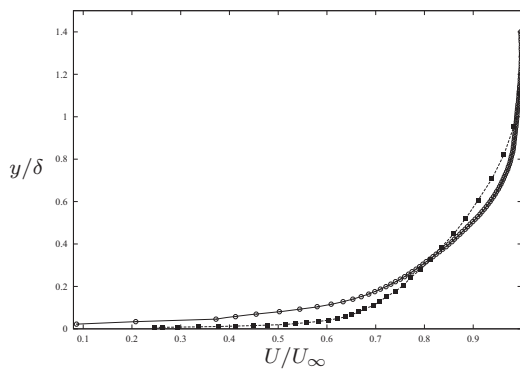


Figure 2: Upstream boundary layer profiles for the two experimental facilities, \circ -water channel ($0.9 < \delta/h < 2.7$), \blacksquare -wind tunnel ($\delta/h = 4$)

RESULTS

The recirculation region dimensions using the PIV results were determined by calculating the streamlines (see equation 2), above the step surface.

$$\Psi = \int_0^y (U/U_\infty) d(y/h) \quad (2)$$

For the data analysis, the Cartesian coordinate system was fixed at the step leading edge. The mean reattachment distance, X_L , occurred where the dividing streamline, $\Psi = 0$, (from here on denoted as Ψ_0) bifurcated at the step surface and the region of negative flow ceased. At the reattachment point, one arm of the dividing streamline returns upstream into the recirculation region and the second continues downstream. The height of the recirculation region is defined as the maximum height of the dividing streamline above the step $Y_b = \Psi_0(y)_{max}$.

A typical mean streamwise velocity, \bar{U} , contour plot obtained from the raw PIV data is shown in figure 3. In figure 3, the flow is from left to right with the length and velocity scales non dimensionalised against the step height, h , and freestream velocity, U_∞ , respectively. The Reynolds number, Re_h of figure 3, is 2 750. The recirculation region is indicated by the solid line while the dashed line encapsulates

the region of entirely negative or backflow. The mean recirculation length, X_L , and height of the recirculation region, Y_b of figure 3 are $1.87h$ and $0.29h$ respectively.

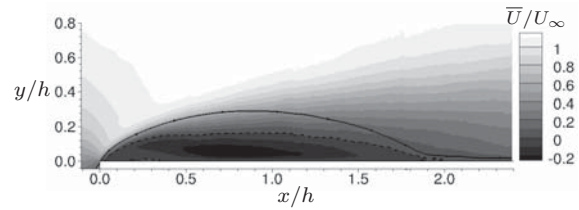


Figure 3: General bluff body flow features of the FFS flow, $\delta/h = 1.35$, $Re_h = 2750$

Figure 3 also displays the region of increased wind speed above the step, beneficial in a wind energy sense. The available power of a wind turbine increases with the cube of the mean wind speed, as shown in equation 3,

$$P_{avail} = \frac{1}{2} \rho A U_\infty^3, \quad (3)$$

where A is the turbine swept area. From equation 3 it follows that a slight increase in wind speed will lead to significant additional energy generation. The maximum wind speed in figure 3 is 21% higher than the freestream wind speed, leading to a 77.2% increase in available power. However, despite a turbine being more profitable in an energy yield sense, the intense velocity shear will subject turbine componentry to dynamic loads.

The free shear layer can be seen from the turbulent velocity component plots of figures 4 and 5. Figure 4 displays the non-dimensionalised streamwise perturbation rms velocity:

$$u_{rms} = \frac{\sqrt{\langle u'^2 \rangle}}{U_\infty}, \quad (4)$$

and figure 5 displays the non-dimensionalised Reynolds shear stress ($\overline{u'v'}/U_\infty^2$) component. Figure 5 shows that the free shear layer expands through turbulent mixing as expected. Turbulent mixing is the principal mechanism promoting reattachment. This mixing entrains higher velocity free stream fluid into the recirculation region to overcome the momentum deficit created by the separation above the step. The maximum u_{rms} velocity occurs just downstream of the step in the free shear layer for all Reynolds numbers. This is a direct result of the bluff body nature of the obstacle. Streamwise perturbations generated by the step in the free shear layer are in the range of 37 to 45% of U_∞ . There is no real trend in the growth of the perturbations but are higher than those reported from previous research for a blunt flat plate (20 -30%) and a normal flat plate (30-34%) in Agelinchaab and Tachie (2008).

The reattachment length was measured in the wind tunnel using surface flow visualisations. Black carbon powder was evenly spread over the step surface prior to starting the tunnel. A region deficient of powder formed where the shear layer impinged onto the step surface at reattachment revealing the reattachment zone as depicted in figure 1.

The variation in reattachment length, X_L , with Reynolds number, Re_h , can be seen in figure 6. The trends for the three different δ/h ratios are indicated by separate trend lines. The large error bars used for the $\delta/h = 4$ results in figure 6 represent the reattachment zone dimensions obtained from the flow visualisations. The mean reattachment,

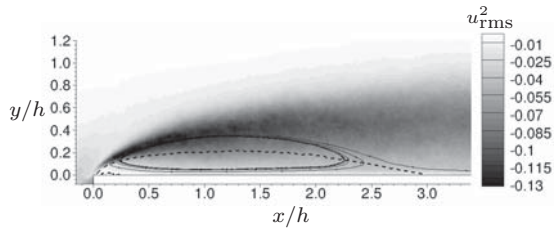


Figure 4: Streamwise perturbations within the shear layer u_{rms}^2 ; $\delta/h = 1.35$; $Re_h = 6741$

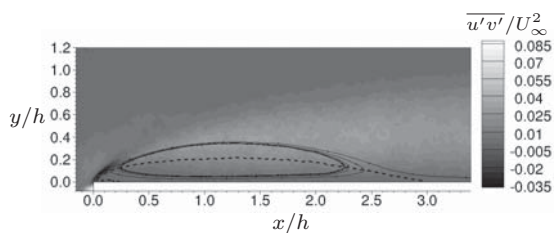


Figure 5: Reynolds shear stress contours $\overline{u'v'}/U_\infty^2$; $\delta/h = 1.35$; $Re_h = 6741$

X_L , for this δ/h ratio was assumed to lie at the midpoint of this zone.

An obvious point to note from figure 6 is that the variation of reattachment length, X_L with Re_h for a given δ/h ratio is monotonic over the entire Re_h range. As Reynolds number increases for a given δ/h ratio, the upstream flow is deflected further into the free stream, elongating the recirculation region. Also, figure 6 reveals the existence of two regimes. The reattachment length becomes less sensitive to increasing Reynolds number beyond $Re_h = 8500$. This behaviour is thought to be due the reduced influence of viscous forces close to the step at higher Re_h values. The greater influence of free stream inertial forces (momentum of free stream flow) at high Re_h encourages the plateau in the results. However, as shown by the spread of results obtained by previous researchers in table 1, results are heavily dependant on several flow parameters.

The change of regimes may also be due to the flow becoming increasingly three dimensional. It has been shown that flow over a forward facing step becomes increasingly three dimensional with decreases in the W/h ratio (Largeau and Moriniere 2007). In the current study with the three step heights simulated, the W/h ratio reduces by a factor of 3 (whilst at all times remaining > 10 ensuring nominally 2D flow).

However, increases in W/h ratio produces more 'branching structures' between the upstream recirculation region and the recirculation region on top of the step (Largeau and Moriniere, 2007). Unlike the Largeau and Moriniere study, which permitted three dimensional flow around the side of the model, here, the experimental models were either fitted with end plates or spanned the entire working section which would emphasise this mechanism to transport fluid from the upstream recirculation region to that downstream. As measurements were only taken at the mid span and in one plane, the current results cannot reveal the three dimensional fluid movement upstream of the step and may form part of future planned research.

When δ/h is less than unity, the free stream velocity will interact with the leading edge of the step directly. The free stream velocity, larger than that within the boundary layer will cause a greater perturbation to the flow field as the flow will be deflected further into the free stream. However, the higher free stream velocity above the free shear layer will contract the increased flow deflection and will suppress the shear layer. In this way as δ/h becomes incredibly lower than unity ($\delta/h \ll 1$) the influence of the upstream boundary layer is reduced and the results will more closely approximate separated flow over a blunt flat plate (Hillier and Cherry, 1981).

Conversely, when δ/h is greater than unity, the flow will be deflected less into the freestream due to the reduced velocity within the boundary layer. In this case, the reattachment length will be affected significantly by an increase in Reynolds number due to the velocity gradient in the boundary layer. The turbulence within the boundary layer will enhance mixing between the free stream and recirculating flow close to the step, promoting reattachment. It is for this reason that results obtained from $\delta/h > 1$ studies are heavily dependant on Re_h as shown in table 1. Variance between previous researchers results can be partially explained by the different boundary layer profiles and length scales therein which would affect the free shear layer dynamics.

The mean reattachment length obtained by Agelinchaab and Tachie (2008), is higher than any X_L obtained at a comparable Reynolds number in the current study. Their open channel setup and high model blockage ratio (22%) introduces free surface effects which have been minimised in the current study. The free surface will act as a momentum sink where the flow acceleration created by the step blockage can be released via surface deformation prolonging separation. Closed channel studies will see a higher velocity and hence greater momentum above the step due to the solid boundaries and the requirement for mass conservation. The higher momentum of the free stream flow will aid in turbulent mixing between the flow within the recirculating region and the free stream leading to earlier reattachment.

A large majority of the previous studies listed in table 1 were conducted on models where the influence of trailing edge separation on leading edge separation cannot be discounted. The question is then whether the experimental model is truly representative of an isolated step. It is suggested that the expansion of the test section at the trailing edge of a model will act as a momentum release prolonging separation and hence effect the free shear layer dynamics at the leading edge. It is for this reason that recirculation regions can form on the short experimental bodies in the Castro and Dianat (1983), Arie et al. (1975) and Bergeles and Athanassiadis (1983) studies.

Interestingly however, flow does not reattach to the top surface of the block geometry investigated in addition to the FFS geometry in the Moss and Baker (1980) study despite having the same dimensions and being conducted at the same Reynolds number as the Castro and Dianat (1983) study. This is clearly a δ/h ratio effect and the mechanism for the difference has been attributed to the turbulence within the boundary layer as outlined earlier. This hypothesis adds another parameter to an already complicated relationship which contributes to the spread of results in table 1.

The offset between results of the same Reynolds number in figure 6 is due to a combined effect of the upstream flow conditions, principally the boundary layer thickness and body geometry effects.

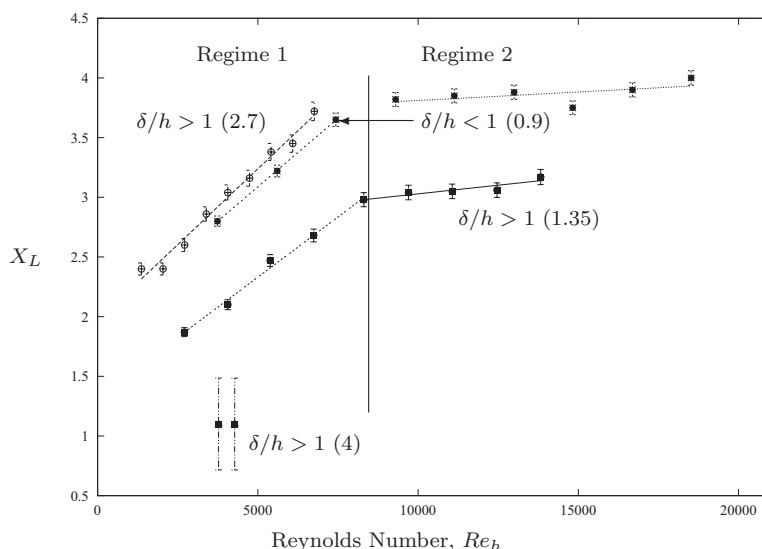


Figure 6: Variation of X_L with Re_h for four δ/h ratios

The surface pressure distribution in the recirculation region was investigated in the wind tunnel to complement the PIV results. A typical mean static surface pressure distribution is shown in figure 7. The pressure coefficient of figure 7 is calculated using equation 5.

$$C_p = \frac{P - P_\infty}{\frac{1}{2}\rho U_\infty^2}, \quad (5)$$

where P is the mean pressure of the tap, P_∞ is the reference freestream pressure, ρ is the density of air and U_∞ is the freestream velocity.

The mean pressure coefficient reduces dramatically downstream of the step face in good agreement with previous researchers where the δ/h ratio is greater than unity (Farabee and Casarella, 1986). There is a noticeable difference between the surface pressure coefficient profiles for different δ/h ratios. For $\delta/h > 1$, the C_p curve monotonically decreases from the step surface however for cases where $\delta/h < 1$, there is a characteristic plateau immediately downstream of the step e.g. Moss and Baker (1980). This plateau is also seen in blunt flat plate studies (Hillier and Cherry, 1981) and hence the absence of such a plateau in the surface pressure distribution can be partially attributed to the enhanced mixing in the boundary layer. The lower velocity in the boundary layer will reduce the suction generated in the recirculation region and lead to a lower minimum pressure coefficient, $C_{p_{min}}$. The minimum pressure coefficient ($C_{p_{min}} = -0.76$) obtained here corresponds very well to that of Farabee and Casarella (1981) ($C_{p_{min}} \approx -0.76$) despite the different Reynolds number and δ/h ratio. As expected the $C_{p_{min}}$ is less than that obtained in the Moss and Baker (1980) study ($C_{p_{min}} = -1.1$). The change in surface pressure distribution with δ/h ratio forms part of the ongoing works.

The mean pressure coefficient at reattachment (C_{p_r}) is indicated on figure 7 by a solid line. C_{p_r} is 55% of $C_{p_{min}}$ which is higher than that obtained by both Farabee and Casarella ($C_{p_r} = 24.5\%$) (1983) and Moss and Baker ($C_{p_r} = 30.8\%$) (1980).

CONCLUSION

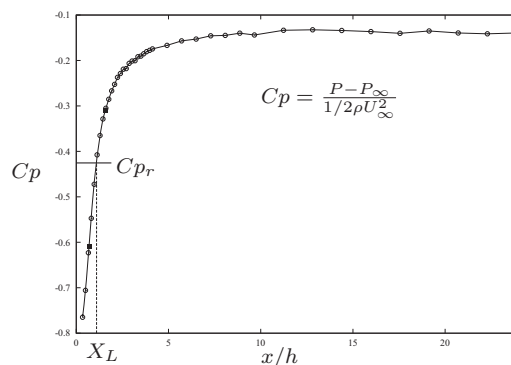


Figure 7: Surface static pressure distribution for $\delta/h = 4$ and $Re_h = 3775$

The recirculation region formed downstream of a forward facing step immersed in a turbulent boundary layer has been investigated using the particle image velocimetry technique. The principal dimension of the recirculation region, the reattachment length, X_L , has been obtained for a wide Reynolds number range and several boundary layer thickness to step height ratios, δ/h . The surface pressure distribution was measured at a single δ/h ratio over a narrow Reynolds number range in a wind tunnel.

The reattachment length tended to increase with Reynolds number for a given δ/h ratio. The range of reattachment lengths obtained in the current study was $1.1h < X_L < 4h$. Two regimes were found to exist in the results. The first regime exists for Reynolds numbers less than approximately 8500, where the reattachment length is heavily dependant on the Reynolds number. Whereas, the second regime exists for Reynolds numbers greater than 8500 with the reattachment length only weakly affected by Reynolds number. Surprisingly, this regime change occurred independently of the δ/h ratio. The regime change is postulated to occur due to a change in the dynamic between the upstream and downstream recirculation regions. The planar nature of the experimental technique employed here could not reveal this change and may form part of the ongoing work in the

area.

The offset between results at the same Reynolds number is due to a combined effect of the upstream flow conditions, principally the boundary layer thickness and body geometry effects. The enhanced local mixing produced by the shear layer above the step and the elevated turbulence intensity within the boundary are thought to be the primary mechanisms promoting reattachment.

The surface pressure distributions obtained in the wind tunnel were similar to those found previously on similar geometries and highlighted some important features of the flow which can be attributed to the δ/h ratio. Most importantly was the reduction in minimum pressure due to turbulent mixing within the boundary layer for flows with a δ/h ratio > 1 .

REFERENCES

- Agelinchaab, M. and Tachie, M.F., 2008, "PIV study of separated and reattached open channel flow over surface mounted blocks", *Journal of Fluids Engineering*, Vol. 130, pp. 1-9.
- Arie, M., Kiya, M., Tamura, H., Kosugi, M. and Takaoka, K., 1975, "Flow over rectangular cylinders immersed in a turbulent boundary layer (Part 2, Flow patterns and pressure distributions)", *Bulletin of the JSME*, Vol. 18-125, pp. 1269-1276.
- Bergeles, G. and Athanassiadis, N., 1983, "The flow past a surface-mounted obstacle", *Journal of Fluids Engineering*, Vol. 105, pp. 461-463.
- Bowen, A.J. and Lindley, D., 1977, "A wind-tunnel investigation of the wind speed and turbulence characteristics close to the ground over various escarpment shapes", *Boundary-Layer Meteorology*, Vol. 12, pp. 259-271.
- Bradshaw, P. and Wong, F.Y.Y., 1972, "The reattachment and relaxation of a turbulent shear layer", *Journal of Fluid Mechanics*, Vol. 52-1, pp. 113-135.
- de Brederode, V. and Bradshaw, P., 1972, "Three-dimensional flow in nominally two-dimensional separated bubbles. I. Flow behind a rear-ward facing step", *Technical report 72-19*, Imperial College of Science and Technology.
- Camussi, R., Felli, M., Pereira, F., Aloisio, G., and Di Marco, A., 2008, "Statistical properties of wall pressure fluctuations over a forward-facing step", *Physics of fluids*, Vol. 20, pp. 075113-1 075113-13.
- Castro, I.P., 1979, "Relaxing wakes behind surface-mounted obstacles in rough wall boundary layers", *Journal of Fluid Mechanics*, Vol. 93, pp. 631-659.
- Castro, I.P. and Dianat, M., 1983, "Surface flow patterns on rectangular bodies in thick boundary layers", *Journal of Wind Engineering and Industrial Aerodynamics*, Vol. 11, pp. 107-119.
- Eaton, J.K. and Johnston, J.P., 1981, "A review of research on subsonic turbulent flow reattachment", *American Institute of Aeronautics and Astronautics Journal*, Vol. 19, pp. 1093-1100.
- Farabee, T.M. and Casarella, M.J., 1986, "Measurements of fluctuating wall pressure for separated/reattached boundary layer flows", *Journal of Vibration, Acoustics, Stress, and Reliability in Design*, Vol 108, pp. 301-307.
- Fouras, A., Lo Jacono, D. and Hourigan, K., 2008 "Target-free Stereo PIV: a novel technique with inherent error estimation and improved accuracy", *Experiments in Fluids*, Vol. 44, pp. 317-329.
- Gasset, N., Poitras, G.J., Gagnon, Y. and Brothers, C., 2005, "Study of atmospheric boundary layer flows over a coastal cliff", *Wind Engineering*, Vol. 29-1, pp. 3-24.
- Hillier, R. and Cherry, N.J., 1981, "The effects of stream turbulence on separation bubbles", *Journal of wind engineering and industrial aerodynamics*, Vol. 8, pp. 49-58.
- Kiya, M. and Sasaki, K., 1983, "Structure of a turbulent separation bubble", *Journal of fluid mechanics*, Vol. 137, pp. 83-113.
- Largeau, J.F. and Moriniere, V., 2007, "Wall pressure fluctuations and topology in separated flows over a forward facing step", *Experiments in Fluids*, Vol. 42, pp. 21-40.
- Leclercq, D.J.J., Jacob, M.C., Louisot, A. and Talotte, C., 2001, "Forward-Backward facing step pair: Aerodynamic flow, wall pressure and acoustic characterisation", *Proceedings of the 7th AIAA/CEAS Aeroacoustics Conference*, Vol 1249, pp. 075113-1 075113-13.
- Moss, W.D. and Baker, S., 1980, "Re-circulating flows associated with two-dimensional steps", *Aeronautical Quarterly*, Aug. 1980, pp. 151-172.
- Zhang, C.X., 1994, "Numerical predictions of turbulent recirculating flows with a k-e model", *Journal of Wind Engineering and Industrial Aerodynamics*, Vol. 51, pp. 177-201.